EXPERIMENTAL EVIDENCE OF DEPARTURES FROM LOCAL THERMODYNAMIC EQUILIBRIUM IN ARC PLASMAS AT REDUCED PRESSURE

By Lothar Klein and Harold J. Babrov

August 1968

Prepared under Contract No. NAS W-1566 by
THE WARNER & SWASEY COMPANY
CONTROL INSTRUMENT DIVISION
32-16 Downing Street
Flushing, New York 11354

[redacted]

NATIONAL AERONAUTICS AND SPACE ADMINISTRATION

EXPERIMENTAL EVIDENCE OF DEPARTURES FROM LOCAL THERMODYNAMIC EQUILIBRIUM IN ARC PLASMAS AT REDUCED PRESSURE

By Lothar Klein and Harold J. Babrov

August 1968

Prepared under Contract No. NAS W-1566 by
THE WARNER & SWASEY COMPANY
CONTROL INSTRUMENT DIVISION
32-16 Downing Street
Flushing, New York 11354

NATIONAL AERONAUTICS AND SPACE ADMINISTRATION

ABSTRACT

A wall-stabilized arc of novel design was tested and used for spectroscopic investigations of departures from local thermodynamic equilibrium (LTE) at reduced pressure. Stable arc operation was achieved in argon, nitrogen, hydrogen, water vapor, and air at pressures as low as 0.01 atm and currents up to 200 A. The spectrometer can view the arc radially(side-on) and axially (end-on). Since a prior investigation had shown the absence of axial temperature and pressure gradients, we used the arc preferentially in the end-on mode, in order to detect intrinsic departures from LTE with a minium of laborious data reduction. The core temperature of an argon arc at 1 atm, 0.1 atm, and 0.01 atm pressure was determined from the measured absolute intensities of atomic and ionic lines. The Planck-Kirchhoff method, based on concurrent emission and absorption measurements was also used, but the accuracy of the temperature derived by this method was considerably less than for the temperature obtained from intensities of optically-thin lines. The electron density in the core of the arc was derived from the measured half-width of H_β.

The existence of LTE was demonstrated at 1 atm pressure; 0.1 atm we corresponded to a transition regime, while at 0.01 atm notable departures from LTE were observed. Although in an argon plasma at 0.01 atm pressure the population over excited states of a given species is still determined by a Maxwell-Boltzmann distribution, the concentrations of different species no longer correspond to thermal equilibrium. In particular, the measured electron density is much lower than the equilibrium density consistent with the temperature derived from the intensity of Ar II lines. In a nitrogen plasma at 0.02 atm pressure we observed a large overpopulation of N_2^+ energy levels.

TABLE OF CONTENTS

EXPERIMENTAL EVIDENCE OF DEPARTURES FROM LOCAL THERMODYNAMIC EQUILIBRIUM IN ARC PLASMAS AT REDUCED PRESSURE

Lothar Klein and Harold J. Babrov

The Warner & Swasey Company, Control Instrument Division

I. INTRODUCTION

A. Development of an Improved Plasma-Source

In order to investigate departures from local thermodynamic equilibrium systematically, and also to determine the experimental conditions most favorable for the accurate measurement of transition probabilities, plasmas of different gases have to be studied over a wide dynamical range of pressures and temperature. The advantages of the wall-stabilized arc (1)* as a source of controlled plasmas are well known; however, most arcs of previous design are unsuitable for operation at reduced pressure and with the exception of prior exploratory work by Klein and Babrov (2), no experiments at reduced pressure using the wall-stabilized arc have been reported in the literature.

We have built a wall-stabilized arc, shown in Fig. 1 and schematically on Fig. 2, which incorporates some significant new design features. Positive arc stabilization is achieved by building each of the six sections comprising the arc channel as a stack of thin, water-cooled copper washers, separated by special insulating spacers. The sections are tapered and separated by quartz rings sealed with O-rings. This arrangement allows radial observation of different arc portions while minimizing arc bulging between sections. The electrode design permits also spectral measurements while viewing the arc "end-on" in the axial direction. Gas flow in the arc is arranged so that only test gas fills the constricted channel; in the electrode chambers, filled with argon as shield gas, the arc is essentially free-burning.

---

* Underlined numbers in parentheses denote references listed at the end of this report.

Experiments have been made with different test gases (H, He, N, air, H_2O, CO, CH_4, CN formed from N and CO), and in all cases the arc operated stably at pressures from atmospheric down to 0.01 atm at currents up to 200 A. Previous attempts to use air as a sample gas in the wall-stabilized arc appear to have failed because of stability problems. The experiments with a water plasma are also noteworthy since the spectrum shows a remarkable stability (of the order of 3% for the peak of the strong lines), and the OH bands around 3000Å are very prominent. The Balmer lines of hydrogen are also excited in the water plasma, which facilitates the plasma diagnostics. This source appears, therefore, to be very promising for studying the transition probabilities of the OH radical, which so far has only been done using flames.

B. Advantage of End-On Measurements

In order to derive the spectral data pertaining to homogeneous arc zones from side-on measurements, spatial scanning of the arc and an Abel inversion (13) of the experimental data are required. Although ideally one obtains by this means the complete radial distribution of emission and absorption data, in practice only the values for the arc core are meaningful. Because of the small contribution of the outer zones to the measured integrated emission and absorption, the attainable accuracy for data corresponding to radial zones close to the arc perimeter is poor. This is especially true for absorption measurements (3). Furthermore, and apart from the experimental inaccuracy, any departure from LTE detected in the outer zones may be spurious in the sense that it is only caused by the steep temperature gradients (4).

From a practical point of view, the required computational effort also has to be considered, and this effort can become very laborious especially when line shapes are studied and an inversion is required for each of a large number of closely-spaced wavelengths above and below the center wavelength of the line.

Although, in view of the foregoing, the experimental advantages of measurements in the end-on mode are obvious, they have only been rarely used by other investigators; mainly because of the following reasons:

1. Since the spectrometer has to view a uniform gas sample, this requires the arc plasma to conform to axial symmetry and to be homogeneous along its axis. The optical path-length must be well defined and the contribution of the end-zones (shield-gas region in our arc) should be small.

2. It must be experimentally feasible to obtain radial temperature profiles of different arc sections, in order to establish the uniformity of the arc core.

3. In the end-on mode the optical depth of the plasma becomes more than an order of magnitude larger than for side-on measurements, and consequently the effect of self-absorption

becomes much more important. This severely limits the usefulness of end-on measurements in the usual situation, where the plasma is at atmospheric pressure and absorption measurements are not made. However, if the absorption is measured, the greater optical depth is a significant advantage since it increases the diagnostic possibilities.

II. APPROACH

A. Validity Test for End-On Measurements

Since we had decided to use the arc preferentially in the end-on mode, its symmetry characteristics and axial homogeneity had first to be established by intercomparing the radial distributions of the emission coefficient** for different arc sections, obtained from an Abel inversion of side-on measurements at each of the five ring-windows. Axial homogeneity of the arc can be considered established, if: (1.) the peak emission coefficients corresponding to the arc core are identical for the five sections and correspond to the geometrical center of the arc channel and, (2.) the emission coefficient of the arc core, derived from side-on measurements, multiplied by the arc length, equals the spectral radiance of the arc core measured directly in the end-on mode. A spectral feature must be used which prior absorption measurements in the end-on mode have shown to be optically thin, in order to rule out the effect of self-absorption.

The usefulness of these measurements is enhanced if the spectral radiances of several spectral features are measured concurrently. Assuming the plasma to be in LTE, the temperature profile of the arc can then be simply derived from the radial distribution of the emission coefficients. Agreement between the temperature profiles obtained from different spectral features is a necessary - but in general not sufficient - condition for the existence of LTE. Further probing into the equilibrium situation requires absorption and line-width measurements, which are more convenient to make in the end-on mode, as explained above.

B. Absorption Measurements

In emission, one measures the intensity of a spectral line, which is proportional to the population of the upper energy level for the transition, while from absorption measurements information is gained on the population of the lower level. The importance of absorption measurements becomes evident when one considers the first four excited levels of the argon atom, belonging to the $3p^54s$ configuration.

** emission coefficient is defined as spectral radiance per unit length

Two of these levels are metastable, transitions from the other two levels to the ground state lie in the experimentally inaccessible vacuum ultraviolet. Therefore, their populations cannot be determined from emission measurements. However, the strong Ar I lines in the near infrared belong to transitions to these levels, thus the steady state distribution between these and higher excited levels can be determined from absorption measurements.

The extreme brightness of arc plasmas poses special experimental problems in the measurement of absorption. An evaluation of available background sources was required, and a high-pressure xenon arc proved to combine the desired characteristics of high intensity and great stability. Our work with the xenon arc has already been published (3) and, therefore, is included in this technical report by reference only.

C. Determination of Plasma Temperature

The radiance of an optically thin spectral line corresponding to a transition between two discrete energy levels, p and q, is proportional to the population density of the upper level p, and the constant of proportionality is given by A(p,q), the Einstein transition probability for spontaneous transitions. If the concentration of emitter is constant over the optical path length, L, we have:

$$I(p,q) = \int_0^L dx \int_{\Delta\lambda} N(\lambda)\, d\lambda = \frac{h\nu_{pq}}{4\pi} A(p,q)\; n(p)\; L \qquad (1)$$

Where $N(\lambda)$ is the intensity as a function of wavelength (the line shape), n(p) is the population density of the upper level, h is Planck's constant, and ν_{pq} is the frequency of the transition. The wavelength interval $\Delta\lambda$ includes the line in question, but no other lines. Therefore, the measurement of line intensity provides essentially a means for determining the population density of the various species (molecules, atoms, ions) present in a plasma. If energy transfer by radiation is small, and dissociation, ionization, and excitation are effected by collisions with electrons possessing a Maxwellian velocity distribution, the population distribution over the different energy levels is also thermal (4). Although over large distances, inhomogeneities (mostly temperature gradients) are usually present, one can define a small homogeneous plasma volume over which the plasma is in local thermodynamic equilibrium (LTE). A plasma in LTE of known chemical composition and pressure is then completely described by its temperature. The population distribution over all species and energy levels can be calculated using the Boltzmann and Saha equations, the ideal gas law, and the conditions of plasma quasi-neutrality. Therefore, when LTE exists n(p), the population of the upper state p, is a unique function of the temperature. There still exist theoretical uncertainties related to collective effects in plasmas (e.g. the lowering of the ionization potential), but these phenomena are of little consequence in plasmas at reduced pressure.

Assuming that LTE exists, we have calculated the populations of the various energy levels as a function of temperature, at different pressures (1, 0.1, and 0.01 atm), using available tables of species concentration and partition functions (5). It is then a simple matter to infer the plasma temperature from a measurement of absolute line intensity, by use of Eq. (1) and the calculated functional relationship between n(p) and the temperature.

Similarly, the plasma temperature can also be derived from the spectral radiance of the continuum, which in the case of argon takes a particularly simple form if the measurements are limited to the visible and infrared part of the spectrum:

$$N_{cont}(\lambda) = 1.63 \times 10^{-31} \frac{\xi(\lambda)}{\lambda^2} \frac{N_e^2}{T^{1/2}}, \quad (2)$$

where N_e is the number of electrons per cm^3 and $\xi(\lambda)$ is a slowly varying function of wavelength.

In the derivation of Eq. (2) it has been assumed that second ionization is unimportant, which is still valid at the highest temperatures reached in our arc. The units of $N_{cont}(\lambda)$ in Eq. (2) are watts $cm^{-3}\ \mu m^{-1}\ sr^{-1}$. It should be noted that, if the weak temperature dependence given by the $T^{-\frac{1}{2}}$ factor is disregarded, the measurement of the continuum intensity is essentially a measurement of the electron density N_e.

The factor $\xi(\lambda)$ appearing in Eq. (2), although not strictly a constant because of a very weak temperature dependence, is not unlike the transition probability for line radiation since it also has to be obtained either from theoretical calculations - which have more the character of estimates - or experimental measurement. Notwithstanding the claim of higher accuracy put forth by various authors, the numerical value of the transition probability for argon lines can in most cases only be considered firmly established to within a factor of 2. Thus for the Ar II 4348Å line, which has been extensively used in this investigation, Olsen (6) has reported a measured value of 1.15×10^8; Garstang (7) has calculated a value of 1.28×10^8, but Popenoe and Shumaker (8), in very careful experimental work more recently determined the transition probability to be 2.4×10^8. Because of the uncertainty in the transition probabilities combined with the inaccuracy inherent in intensity measurements, n(p) or n(p)/n(p') (if the ratio of line intensities is used) must be very sensitive functions of temperature if reasonable accuracy in the measured temperature is to be attained.

Because the spectrum of atomic argon does not contain lines lying in the same spectral region but emitted from levels with reasonably large energy gaps, the otherwise appealing method of measuring temperature from the relative intensities of spectral lines, called Boltzmann plot method (2), is inherently so inaccurate as to be practically useless for precision work. The small gain in accuracy by using lines in different spectral regions (requiring a change of detector) is mostly nullified by the increased inaccuracy of intensity measurements under these circumstances. In this investigation we have used either the absolute intensity of atomic and ionic lines or the ratio of the intensity of an atomic line to that of an ionic line. The energy gap is very large, so the ratio of intensities between atomic lines and ionic lines of the same atom is a very sensitive function of the temperature. An error estimate can be made from Table I.

TABLE I

Fractional Intensity Increment for a Temperature Increment of 100°K at a Temperature of 12,000°K (argon plasma at 1 atm).

I (Intensity or Intensity Ratio)	$\Delta I/I$ for ΔT = 100°
Absolute Intensity of Ar I 4345Å	32%
Absolute Intensity of continuum at 4345Å	34%
Absolute Intensity of Ar II 4348Å	60%
Intensity Ratio of Ar II 4348 / Ar I 4345	38%
Blackbody Intensity at 8115Å	1.5%

It follows from Table I that around 12,000°K an error of 100% in the intensity of the ionic line due to the use of incorrect transition probabilities induces an error of only 1.4% in temperature when the absolute intensity of the ionic line is used to determine the temperature. This error is not large. The method based on the intensity ratio of the ionic and atomic line offers, however various advantages for our investigation, notwithstanding its smaller sensitivity:

1. Since the detector response is flat over a few Angstroms, in principle no intensity calibration is required and the temperature can be derived simply from the measured signal ratio,

2. Because of their close proximity, both lines can be quickly scanned, avoiding errors due to temporal arc variations,

3. Knowledge of the optical path length is not required, which is important for end-on measurements. In fact, a self-consistency check can be made by first deriving the temperature by this method and dividing the measured absolute intensity of each line by the calculated intensity at this temperature. If essentially the same factor is obtained for both lines and this factor is close to the geometrical length of the arc seen by the spectrometer, it can be assumed - unless one has an unlikely case of compensating errors, - that the arc is uniform along its core and that neutrals and ions are in a Saha equilibrium.

The last entry in Table I refers to the Planck-Kirchhoff method (see e.g. Ref. (3)) using the measured peak emission and absorption of Ar I 8115Å. It is obvious that this is a poor method, especially in the case of low absorption (say around 10%), where measurement errors as large as 20% can easily occur, leading to errors in temperature of more than 1000°K. This explains the large data scatter which we obtained in the measurements of the argon arc at 0.1 atm pressure (see Section IV C).

D. Line Intensity Peaking by Arc Current Variation

In an LTE plasma, the population of excited states relative to the total number density of particles of the same species is given by the Boltzmann factor, which increases monotonically with temperature. Increasing temperature, however, also affects the total number density because of dissociation or ionization losses. The number density of emitters reaches a maximum at a certain temperature calculable from theory - the "normal" temperature - beyond which it decreases again.

The Fowler-Milne method, introduced in arc-plasma diagnostics by Larenz (9), uses this fact to determine the temperature profile of an optically thin arc-plasma, if the radial intensity distribution for a line is peaked off the arc center. This method is important because no prior knowledge of the transition probability is required; in fact, it should be possible to derive both the temperature and the transition probability from such a measurement. The usefulness of this method is impaired in practice, however, since small experimental scatter in the measured intensities may induce a spurious off-axis peak in the inverted data and lead to temperatures which are much too high. For instance, Olsen (10) has pointed out that his previously reported measurements were vitiated by an inaccurate use of the Larenz method, and the high temperature of an RF arc as determined by Reed (11) appears to be strongly affected by this error.

The difficulty of false off-axis peaks can be avoided in end-on measurements, since variation of the arc current provides a simple means of changing the core temperature while changes in the intensity of a spectral line can be directly observed on the recorder display. Provided the arc can be run at a current large enough to exceed the normal temperature, it is then possible to adjust the arc current accurately and unambiguously for peak intensity of the spectral line. If the spectrum of the arc core is measured at this value of the arc current, we then know that its temperature equals the normal temperature for the "thermometer line".

Although in end-on measurements the effect of spurious off-axis peaks can be avoided, in practice it is still not a good method to determine the plasma temperature, since close to the normal temperature the spectral radiance of a line is in general a very insensitive function of temperature (see Figs. 12 and 14). The line-peaking method has, however, many advantages when studying departures from LTE and has been applied repeatedly in this investigation. Since in an LTE plasma the peak spectral radiance is a unique function of pressure alone (which can easily be measured), departures from LTE become immediately evident if the discrepancy between measured and calculated peak intensity is larger than can be explained by uncertainties in the transition probabilities.

III. EXPERIMENTAL

Figure 3 shows the experimental set-up, and in Fig. 4 the optical system used for concurrent measurements of emission and absorption is shown schematically. The spectrometer was a 1.5m Czerny-Turner instrument built in this laboratory. Because the light beam had to be stopped down to small apertures, only a small portion of the large ruled area (150 x 206 mm) of the available grating was actually used. The grating, blazed for a first order wavelength of 6μm, was used in higher orders; discrimination against unwanted orders was effected by a hind-prism (shown in Fig. 3 with the cover removed). The detector was either an RCA 1P21 or 7102 photomultiplier, and the spectrum was displayed by a strip-chart recorder after synchronous rectification of the chopped signal. For absorption measurements, light from the cathode spot of a high-pressure xenon arc, run at 2.2 kW electrical power input, was focused on the arc plasma and passed through the arc plasma to the entrance slit of the spectrometer. By selectively modulating the Xe-arc background source with the absorption chopper (CH_2 in Fig. 4), fairly accurate absorption measurements could be made even when the spectral radiance of the arc plasma was considerably stronger than the background source.

For intensity calibration, a tungsten strip-lamp was imaged on the entrance slit by rotating a mirror. Since both light path and window transmission losses were identical for arc and strip-lamp, calibration was simplified. A combination of field stops (entrance slit masks) and aperture stops (masks on the imaging mirror shown in Fig. 4) ensured that only light from uniform plasma regions fell on the detector. In most cases the slit height was limited to 0.25 mm and the aperture for end-on measurements to f/135. An experimentally calibrated set of larger aperture stops was used for the intensity calibration with the strip-lamp, since otherwise the strip-lamp signal was mostly too weak. This technique is preferable to increasing the slit height or width, since the sensitivity of the detector is in general not uniform over its surface.

The wall-stabilized arc was mounted on an x-y table (precision 0.01 mm), either horizontally for end-on measurements, as shown in Fig. 3, or vertically for side-on measurements. It was thus possible to refer the lateral intensity profile, obtained by spatially scanning the arc in the side-on mode at the location of the five ring-windows, to the geometrical axis of the arc channel.

Electric power was supplied by a pack of three Miller welder rectifiers with line voltage compensator and ripple filter. Because of their excellent stability (3) recourse to elaborate current monitoring systems, as used by other investigators (8) did not appear to be justified. Their versatility in open circuit voltage setting (75-900V) is a positive advantage, since optimum operation was achieved when the O.C.V. was approximately three times the operating arc voltage. The wall-stabilized arc was efficiently cooled with distilled water (to minimize side-arcing) under 5 atm pressure, recirculated through a heat exchanger cooled with city water.

The arc was always started at atmospheric pressure while being flushed with argon, by introducing and quickly withdrawing a thin (4.8 mm diameter) tungsten rod. Since the arc electrodes were also of tungsten, carbon impurities were completely avoided. For operation at lower pressures, the arc was evacuated with a pump of large capacity (Kinney KDH 150). Operation at pressures as low as 0.01 atm posed no special problems, since at lower pressures the gas flow also can be reduced.

The gas flow pattern is shown schematically in Fig. 2. Shield gas was admitted at two ports in each electrode chamber to effectively shield the electrodes; test gas was introduced into the arc channel at two symmetrically positioned ports. The gas ports were designed for uniform tangential inflow around the arc perimeter, such that a weak vortex field was induced. The six gas flows were independently monitored by precision rotameters. No gas was blown in or out at the midpoint of the arc channel seen by the middle ring window, and this was the location of a pressure tap. A mercury manometer and a Wallace & Tiernan Bourdon gauge were connected to the pressure tap. The Bourdon gauge was used to get accurate readings in the range 0-20 torr, and the manometer was used to measure pressures higher than 20 torr.

For quiescent arc operation, the flow of shield gas had to be considerably higher than the flow of test gas, but as long as the flow regime was balanced, the arc parameters and the measured spectral intensities were quite insensitive to relatively large changes in gas flow. When pumping the arc down from 1 to 0.01 atm, the flow rates could be reduced approximately by a factor of five, and the total flow rate of test gas was then of the order of 70 cc/min, while the flow of shield gas was typically an order of magnitude larger. The low flow rate required for the test gas in the evacuated wall-stabilized arc can be contrasted with prior work at reduced pressure using a gas-vortex stabilized plasma-jet, where the required flow rate was three orders of magnitude higher (2).

To check for pressure gradients in the arc, we measured the pressure at different locations in the arc. For this test the current was 62A, argon was the shield gas, and nitrogen was the test gas. The argon flow was more than ten times the flow rate of nitrogen. The measured pressure was 6.9 torr at the midpoint of the channel, 6.2 torr in the cathode chamber, and 5.5 torr in the anode chamber. This demonstrates the absence of pressure gradients due to the flow field, but the slightly higher pressure in the confined channel - notwithstanding the smaller flow rate - can only be attributed to the self-magnetic compression effect (12). In the scheme used by us, the arc burning in shield gas is purposely unconfined, to weaken the Lorentz force, since this force directed axially inward, combined with the opposing flow, might induce penetration of shield gas into the arc channel and even bending of the arc ("sausage asymmetry"), as observed in an arc of older design (2). A special geometry was also chosen for the cathode (see Fig. 2), so that the cathode jet is deflected and does not impinge on the plasma in the arc channel.

It is a distinct advantage of the wall-stabilized arc as compared with other sources that for an argon arc at a given pressure the plasma regime (e.g. the temperature profile) is determined by only one external parameter, the arc current. At a fixed current setting, the reproducibility of the core temperature for an atmospheric argon arc was better than within 1.5% (as determined by the variations in line intensities from run to run). Over a run the temperature could mostly be kept constant within 0.5%.

IV. MEASUREMENTS AND RESULTS

A. Side-On Measurements of the Argon Arc at 1 atm

The three contiguous spectral features: Ar I 4345Å, Ar II 4348Å, and the continuum at 4350Å were used for this study. Absorption measurements in the end-on mode had shown these features to be optically thin (peak absorption less than 3%). The measurements were done at an arc current of 76A. The arc was set up in the vertical position and its axis accurately aligned with the y-axis of the slide table. The intensity of the three spectral features was recorded while the midplane of one of the five ring windows was traversed across a position optically conjugate to the entrance slit of the spectrometer. The arc was then moved vertically to bring the next window in focus and the traverse repeated. Thus we obtained for each of the three spectral features the intensity distribution corresponding to the different arc sections seen through the ring windows. Figure 5 shows such a plot of the intensity distribution for the middle window. The intensity dip of a few percent near the center of the distribution was typical for most measurements and has also been observed in prior work (2). It appears to be caused by reflection effects and is not of particular significance. The center of the lateral intensity distribution was found from these plots by folding (23), and the position of the arc center relative to the geometrical center of the arc channel was thereby determined. In all cases, both centers were coincident within the estimated experimental accuracy (about 0.2 mm).

Barr's method (13) was used for the Abel inversion of the lateral intensity distribution into a radial profile for the emission coeffiecient (see Fig. 6), and finally the temperature profile of the arc at the different arc sections was derived as explained in Section II C. For the continuum intensity at 4350Å we used Wende's experimental value of $\xi(\lambda) = 2.05$ (14) which agrees to within a few percent with theoretical calculations by Schlueter (15) and Biberman (16). For the Ar I line at 4345Å we used $A = 2.8 \times 10^5$ sec^{-1} (17), and for the Ar II line at 4348Å we used Popenoe and Shumaker's value of $A = 2.4 \times 10^8$ sec^{-1} (8).

Figure 7 shows the temperature profile for different sections of the arc, as derived from the continuum intensities. Only one profile is shown for each pair of symmetrically positioned windows since the differences were only small and of the same order of magnitude as the experimental scatter in the data. Although not of large magnitude, there are, however, noteworthy differences between the three profiles shown, corresponding to different gas flow regimes. In the midplane of the arc (window 3), where no gas flows in or out, the core temperature is slightly higher (by about 100°K) and its profile is flatter and broader, caused by the bulging of the arc. The slight gas inflow at the location of window 2 and 4 decreases arc bulging, leading to a steeper temperature profile, but has only a small effect on the core temperature. At the lip of the arc channel (windows 1 and 5) the core temperature had not changed, but the temperature decreases more rapidly towards the periphery. It follows from these profiles that the arc core (defined as the arc region over which temperature variations are of the order of 1%) is axisymmetric and has a diameter of about 1 mm.

The temperature profiles of the same arc section as obtained from the three spectral features corresponding to different degrees of freedom are compared in Fig. 8 (window 3) and Fig. 9 (window 4). It appears that the temperature profiles agree within the experimental accuracy.

B. End-On Measurements of the Argon Arc at 1 atm

In order to complete the validity test for end-on measurements (see Section II A), the spectral radiance of the three spectral features used for side-on measurements was also measured in the end-on mode. For the arc operating at a current of 76A the following effective pathlengths, L*, were obtained by dividing the spectral radiance (end-on) by the peak emission coefficient (side-on):

1) L* = 11.5 cm from the continuum intensity at 4350Å
2) L* = 10.0 cm from the intensity of the Ar II line at 4348Å
3) L* = 13.8 cm from the intensity of the Ar I line at 4345Å

Within the measurement accuracy, L* agrees with the physical length of the confining channel, which was 10 cm. The total distance between electrodes was 14 cm, but the contribution of the unconfined end-zones appears to be small, especially at the cathode end, where the arc is deflected downward out of the narrow solid angle accepted by the monochromator.

The core temperature of the atmospheric argon arc corresponding to other values of the arc current was obtained in the end-on mode from the intensity ratio of Ar II 4348 and Ar I 4345. The effective pathlengths L* were also calculated to check for self-consistency. In some cases L* turned out to be considerably smaller than 10 cm, but the discrepancy could always be traced to an incorrect arc alignment (arc alignment is critical for this type of measurement), and these measurements were discarded.

We also determined the core temperatures independently by the Planck-Kirchhoff method, using the strongly absorbing Ar I 8115 and Ar I 8104 lines. In Fig. 10 a typical emission-absorption record is shown.

In Fig. 11 the core temperatures as calculated by the Planck-Kirchhoff method (solid circles) and by the ratio of Ar I to Ar II line intensities (open circles) have been plotted as a function of arc current. The solid circles are shown as pairs with a vertical line between each pair to show the experimental scatter of these temperatures calculated by the Planck-Kirchhoff method. The experimental scatter of the temperatures calculated from the ratio of intensities of the Ar I and Ar II lines were too small to plot on this graph. It is evident from this figure that the temperature derived by the intensity ratio method is more reliable, since this is a more sensitive method. The temperature derived by the Planck-Kirchhoff method shows considerable experimental scatter and the discrepancies between the temperatures measured by these two different methods can hardly be attributed to departures from LTE.

In the case of the atmospheric argon arc, the electron density could not be conveniently determined from the half-width of the H_{β} line, since the total width of this line was larger than the bandpass of the order-sorting prism spectrometer (determined by the free spectral range in the 12th grating order). We used the measured halfwidth of Ar I 4345 (1.29Å, measured with a spectral slitwidth of 0.2A) to derive for the 76 ampere arc an electron density of 5.2×10^{16} based on Griem's tables (18). This corresponds to an equilibrium temperature of 11,650°K in good agreement with the temperature derived from line intensities.

Finally, the 76 ampere argon arc in the end-on mode was used to determine the transition probabilities of a few atomic lines in the blue region of the spectrum. These transition probabilities are presented in Table II below.

TABLE II

Transition Probabilities For Some Ar I Lines

Line	This Work	Gericke (17)	Olsen (6)	Popenoe (8)
	$A \times 10^{-5}$ (sec^{-1})			
Ar I 4259	28		24.6	44
Ar I 4266	2.4	2.8		
Ar I 4272	6.1	7.1	3.68	9.4
Ar I 4300	2.7	3.4		4.1

The accuracy of our values is estimated to be not better than ± 30%, but they offer evidence in support of Gericke's values. The transition probabilities derived by Popenoe and Shumaker appear to be too high.

C. The Argon Arc at Reduced Pressure

Lowering of the arc pressure has a striking effect on the appearance of the argon spectrum. The reduction of the electron density leads to a marked decrease of the continuum intensity (proportional to N_e^2, see Eq. 2), such that at 0.01 atm the continuum was everywhere too weak to be measurable. Stark broadening, which is the leading mechanism for line broadening at atmospheric pressure, is depressed and the lines become much narrower. Because of these two phenomena, discrimination against overlapping lines and spectral background - a source of considerable error at higher pressures - is much simplified. At 0.01 atm the widths of the atomic lines (which are broader than the ionic lines) were always smaller than the relatively narrow spectral slitwidths used, so that the integrated intensity could be inferred directly from the recorded peak signal, avoiding laborious planimetering of line areas on the strip chart record.

It follows from the equilibrium relations for plasmas that at constant temperature a decrease of pressure alone should lead to an increase of the degree of ionization. This effect was clearly observed, and at 0.01 atm pressure the atomic argon lines in the visible were too weak to be measured, since the Rowland ghosts of neighboring strong Ar II lines were of comparable strength. Visually one notices that the arc acquires a deep blue color due to the prominence of the Ar II lines in the blue region of the spectrum. Representative spectra showing the effect of lowering the pressure have been presented in Ref. 2.

Measurements were made in the end-on mode at 0.1 atm and around 0.01 atm pressure. Although the stability over a particular run was mostly quite good, the line intensities - especially of Ar II lines - measured in different runs at the same arc current and pressure, showed often notable discrepancies. This is again attributed to arc misalignment, which at reduced pressure can actually lead to an increase of measured line intensity. This effect occurs if radiation from the "cathode spot" (a small inhomogeneous region of higher temperature surrounding the cathode, which expands at reduced pressure) is seen by the spectrometer. In two concordant measurements at 0.1 atm and 80A, which met the self-consistency test ($L^* \approx 10$ cm), we determined from the intensity ratio of Ar II 4348 and Ar I 4345 a core temperature of 13,500 ± 300°K. This temperature was consistent with the measured intensity of a number of other Ar I and Ar II lines in the spectral range 4200 - 5000Å. The temperatures derived by the Plank-Kirchhoff method are shown in Table III.

TABLE III

Core Temperatures of an Argon Arc at 0.1 atm Pressure derived by the Plank-Kirchhoff Method using Two Strong Ar I lines in the Infrared.

Arc Current (A)	Line	Peak Absorption (%)	Temperature (°K)
70	8104	9	12,600
	8115	15.2	12,700
80	8104	9	13,600
	8115	15.7	15,600
90	8104	11.5	13,700
	8115	21.5	12,900

Table III indicates the noise in the data, and absolute errors in measured absorption of the order of 4% could easily have occurred which would lead to errors in temperature of the order of 2000°K (see Section II C). It is not assumed that a real discrepancy exists between the temperature derived from intensities of optically thin lines (which is a much more sensitive method) and from emission-absorption measurements.

A notable discrepancy was observed in the measurement of the electron density from the half width of the H_β line. Three independent measurements for different runs at 0.1 atm and 80A gave a value for the electron density, N_e, of $(1.30 \pm 0.1) \times 10^{16}$ cm^{-3}. For an Argon plasma at 0.1 atm pressure and in LTE, this electron density corresponds to a temperature of 11,700°K, while the electron density at 13,500°K is 2.25×10^{16} cm^{-3}. The results of the continuum measurements, although not completely unambiguous, appear to support the electron density derived from H_β. It should be noted, however, that from 13,500°K to 11,700°K the intensity of ion lines, as calculated from theory, drops by more than an order of magnitude. Therefore, our measurements of the intensities of Ar II lines cannot be reconciled with the equilibrium temperature derived from the measured electron density.

TABLE IV

Core Temperature of an Argon Arc at 0.01 atm Pressure and 80A Current, derived from the Absolute Intensities of Ar II Lines.

Line	E_n (eV)	A x 10^{-8} (sec^{-1})	Ref. for A	Temperature °K
4806	19.14	0.79	(6)	14,300
4848	19.22	1.1	(18)	14,200
4352	19.22	0.092	(18)	14,400
4348	19.41	2.4	(8)	14,200
4880	19.60	0.66	(6)	14,200
3588	22.85	3.0	(18)	14,400
3576	22.92	2.5	(18)	14,500
3548	23.00	0.8	(18)	14,500
3559	23.06	2.7	(18)	14,500
3561	24.52	3.0	(18)	14,500

In Table IV, the core temperatures of an Argon arc at 0.01 atm pressure and 80 A arc current derived from selected Ar II lines are presented. In most cases the transition probabilities calculated by Griem (18) have been used, since they give consistent results. If we had used Olsen's value (10) for Ar II 3588, which is smaller by a factor of five, this line would have given a temperature higher by about 2000°K. Our measurements, therefore, seem to support the theoretical transition probabilities for the UV lines.

Of particular interest are the measurements of the strong Ar I lines in the near IR. At a pressure of 0.01 atm these lines were found to be optically thin. The intensity of Ar I 8104 and 8115 were measured at different arc currents between 50 A and 150 A, but no intensity variation larger than the noise in the data (less than 30%) was observed. Furthermore, for an 80 A arc, the signal increase observed when sitting on these lines and increasing the aperture from f/135 to f/50 corresponded exactly to the signal increase measured with a source of uniform brightness. Using the value of A = 0.22 x 10^8 sec^{-1} (6, 19) for the Ar I 8115 line, and assuming L = 10 cm, the measured intensity for this line corresponded to the peak of the population for the upper level of the transition ($2p_9$) for an argon plasma at 0.01 atm and in LTE. The calculated variation of the population of the $2p_9$ level with temperature is shown in Fig. 12 and it can be seen that in the neighborhood of the maximum it is a slow varying function of temperature. The experimentally established constancy of the population over most of the arc cross section and over a wide range of arc current would indicate - within the LTE assumption - a temperature range of 11,000 to 13,000°K under all investigated conditions. Identical results were derived from the measured intensity of Ar I 8104.

In the run at 0.01 atm pressure and 80 ampere current, the half-width of H_β was 2.25Å, as measured with a spectral slit width of 0.8Å. We correlate this measurement with an electron density of $(7 \pm 1.5) \times 10^{14}$ cm^{-3} which, at LTE, corresponds to a temperature of 9300 ± 200°K. In a plasma in LTE, the electron density at 0.01 atm is almost constant - $(2.6 \pm 0.1) \times 10^{15}$ cm^{-3} - from 11,500°K to 14,500°K, but four times higher than the value calculated from the half-width of the H_β line. On the other hand, if we accept the temperature corresponding to the measured electron density, the measured intensity of the ion lines would be almost three orders of magnitude larger than calculated for the LTE model.

D. The Nitrogen Arc at Reduced Pressure

Some exploratory experiments were made with nitrogen as a test gas, at a pressure of 0.02 atm. The arc was viewed in the end-on mode. The spectrum of the arc core is dominated by closely-spaced rotational lines belonging to the N_2^+ (1st negative) system. The strongest band corresponds to the (0,0) vibrational transition, and Fig. 13 shows the spectrum of this band, recorded at an arc current of 40 A and with a spectral slit width of approximately 0.15Å. It can be noticed that the expected intensity alternation due to the effects of nuclear spin (20) is apparent only at the long wavelength side of the band origin, but is smeared out towards shorter wavelengths. This is explained by the fact that strong P-lines overlap strong P-lines and weak P-lines overlap weak P-lines, while in the R-branch the overlap is between strong P-lines and weak R-lines, and vice versa. Only the P(26) line which falls on the band origin is not overlapped by a line belonging to the same band (0 <—> 0 transitions are forbidden), and therefore, this line was selected for measuring the spectral radiance of an individual rotational line. The intensity of this line changed very slowly with increasing current but went through a maximum at a current of 40 amperes.

The end-on spectrum of the 40 ampere nitrogen arc was scanned from 3700Å to 1μ. Only molecular bands appear in the visible, but in the infrared around 9000Å, three N I lines were strong enough for their intensities to be measured. The atomic Boltzmann plot for these lines gave a temperature of 8650°K, although the precision of this method is not very high due to the relatively small difference in upper energy levels. Much better accuracy can be expected if the temperature is derived from the absolute line intensity, which is a very sensitive function of temperature (see Fig. 14). The following temperatures were thus derived from the three lines: 8800°K, 8450°K, and 8700°K. The average of these temperatures is again 8650°K.

The absolute intensity of N I 4110Å - the strongest atomic line in the range of the 1P21 photomultiplier - was calculated assuming a temperature of 8700°K, and compared with the measured absolute intensity of P(26). The latter turned out to be an order of magnitude stronger and this explains why the visible atomic lines do not stand out in the spectrum but are overlapped by closely-spaced rotational lines of comparable or stronger intensity. A temperature of 8700°K is also consistent with the peak temperature for the P(26) line (Fig. 14).

Although so far no indication of a departure from LTE had been found, a marked inconsistency appeared when the maximum value at 0.02 atm for the absolute intensity of the P(26) line was calculated and compared with the measured value: the measured intensity of P(26) is 250 times larger. The theoretical value was calculated as follows: The general expression for the intensity of an optically thin line in an electronic band of a diatomic molecule is

$$I^{n\ v'\ J'}_{m\ v''\ J''} = \frac{hcL}{4\pi\lambda} \frac{\omega_\Lambda\ \omega_I\ (2S+1)\ N_o}{Q_{nuc}\ \ Q_{int}} A^{n\ v'}_{m\ v''} S^{J'}_{J''}\ e^{-E(n,v',J')/kT} \quad (3)$$

where ω_Λ is the statistical weight due to orbital electronic angular momentum (Λ degeneracy), ω_I is the statistical weight due to nuclear spin, the factor (2S+1) is the statistical weight due to electron spin, and N_o is the total number density of the molecular species. The energy of the upper state is given by

$$E\ (n,\ v',\ J') = \left[\nu_{oo} + G_o\ (v') + F_v\ (J')\ \right] hc \quad . \qquad (4)$$

$A^{n\,v'}_{m\,v''}$ is the transition probability for the given electronic band, n v' ⟶ m v''. $S^{J'}_{J''}$ is the angular part of the transition moment (the rotational line strength). Q_{nuc} and Q_{int} are the nuclear and internal partition functions, respectively. For the special case of the N_2^+ band studied (the v' = 0 ⟶ v'' = 0 band of the $B^2\Sigma \longrightarrow X^2\Sigma$ system) Eq. (3) can be simplified.

The integrated spectral radiance of a P(K=even) line of the (0,0) N_2 (1st neg.) band is then given by, (in W cm^{-2} sr^{-1})

$$I\left[(0,0)N_2^+;\ P(K\text{=even})\right] = 1.58 \times 10^{-20} L\ 2K\frac{6}{9}\ \frac{1.24 \times 10^7}{\lambda(\mu)}\ \frac{N_o}{\frac{1}{2}Q_{int}} \times e^{-E(n,\ 0,\ K-1)/kT} \qquad (5)$$

The transition probability due to Bennet & Dalby (21) has been used, the number density and partition function of N_2^+ were taken from Ref. 5, although the value for Q_{int} was found to depart only insignificantly from Q_{int} calculated assuming a simple rigid rotator-harmonic oscillator model.

Because of the overlapping of lines, the intensities of most rotational lines cannot be measured to the accuracy necessary for a meaningful molecular Boltzmann plot. We calculated, however, from theory the intensity of several line blends, assuming a temperature of 8700°K. In all cases the measured and calculated intensities agreed within the experimental accuracy. The attempt to measure the electron density from the width of H_β failed, because of experimental difficulties in admixing a very small, controlled flow of hydrogen.

The experiments with the nitrogen arc at 0.02 atm were repeated in the side-on mode (middle window in focus) with a low-resolution spectrometer. The arc current was varied while sitting on the band head of the (0,0) N_2^+ (1st neg.) band. Again only a surprisingly small change in intensity (a few percent) was measured while the arc current was raised from 80 A to 135 A (or20 kW power input). No atomic lines were found in the visible spectrum of the 135 ampere arc.

V. CONCLUSIONS

Our results give clear evidence of departures from LTE in arc plasmas at reduced pressure, but further work is required before it can be attempted to explain the observed phenomena by a consistent theory. It appears that although the distribution over the energy states for a given species can be described by a certain temperature (i.e. is given by the Maxwell-Boltzmann law), the steady-state concentrations of different species in a plasma at low pressure are no longer in thermal equilibrium. Over-population of metastable levels has been invoked to explain departures from LTE in argon plasmas at reduced pressure (22). Our emission and absorption measurements of the line pair Ar I 8105Å and Ar I 8115Å do not sustain this assumption, since no enhancement was found for the transition - Ar I 8115 - whose lower state is metastable.

Since the concentration of species in a plasma can no longer be calculated from equilibrium relations, low-pressure plasmas are ill suited to determine absolute transition probabilities, but in many instances it can be advantageous to determine relative transition probabilities from measurements at reduced pressure, which can readily be put on an absolute scale if the transition probability for only one line belonging to the same species is known. The usefulness of low pressure plasmas for this work stems firstly from the fact that a higher precision in measured line intensities can be achieved (because of the suppression of overlapping lines and the continuum spectrum), and secondly, on can more readily approach the favorable regime close to the normal temperature where large errors in temperature have only a small effect on the accuracy of the determined transition probability.

REFERENCES

1. J. B. Shumaker, Rev. Sci. Instr. 32, 65 (1961).
2. L. Klein and H. J. Babrov, Technical Report ARL 65-92 (May 1965).
3. L. Klein, Appl. Optics 7, 677 (1968).
4. H. R. Griem, Phys. Rev. 131, 1170 (1963).
5. K. S. Drellishak, D. P. Aeschliman and A. B. Cambel, Technical Report AEDC TR 64-12 (January 1964).
6. H. N. Olsen, J. Quant. Spectry. Radiative Transfer 3, 59 (1963).
7. R. H. Garstang, M. N. Roy Astr. Soc. 114, 118 (1954).
8. C. H. Popenoe and J. B. Shumaker, J. Res. NBS 69A, 495 (1965).
9. R. W. Larenz, Z. Physik 129, 327 (1951).
10. H. N. Olsen, in Temperature, Its Measurements and Control in Science and Industry, Vol. 3, Part 1, Eds. Herzfeld and Brickwedde, Reinhold, New York (1962).
11. T. B. Reed, J. Appl. Phys. 32, 821 (1961).
12. H. Maecker, Z. Physik 141, 198 (1955).
13. W. L. Barr, J. Opt Soc. Am. 52, 885 (1962).
14. B. Wende, Z. Physik 198, 1 (1967).
15. D. Schlueter, Z. Astrophysik 61, 67 (1965).
16. L. M. Biberman, G. E. Norman, and K. N. Ulyanov, Opt and Spectr. 10, 297 (1961).
17. W. E. Gericke, Z. Astrophysik 53, 68 (1961).
18. H. R. Griem, Plasma Spectroscopy, McGraw-Hill, New York (1964).
19. L. R. Doherty, PhD Thesis, University of Michigan (1961).
20. G. Herzberg, Molecular Spectra and Molecular Structure, I Spectra of Diatomic Molecules, Van Nostrand, New York (1950).
21. R. G. Bennet and F. W. Dalby, J. Chem. Phys. 31, 434 (1959).
22. L. E. Brewer and W. K. McGregor, Phys, Fluids 5, 1485 (1962).
23. M. P. Freeman and S. Katz, J. Opt. Soc. Am. 53, 1172 (1963).

LIST OF ILLUSTRATIONS

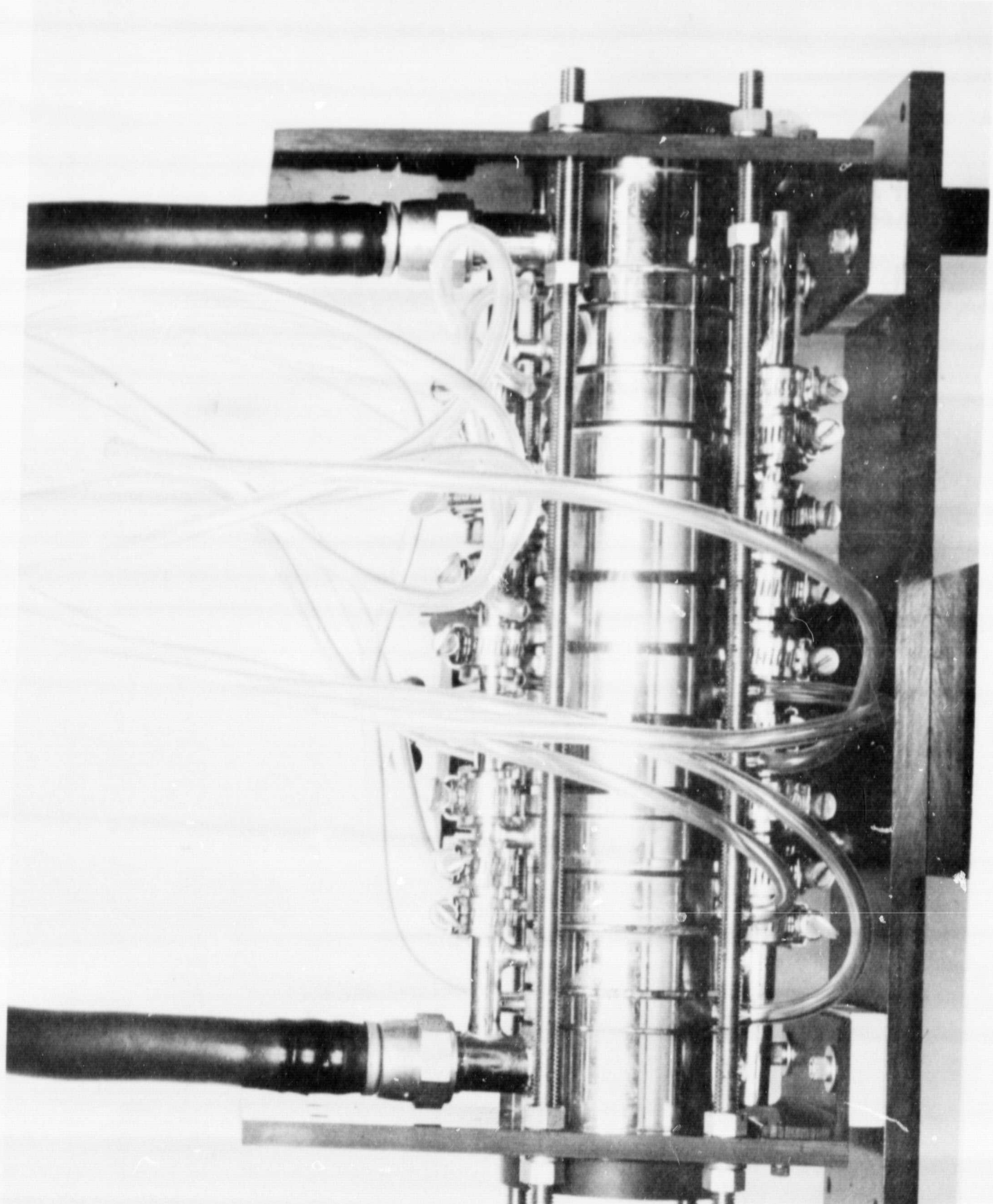

Fig. 1 Side view of the wall-stabilized arc.

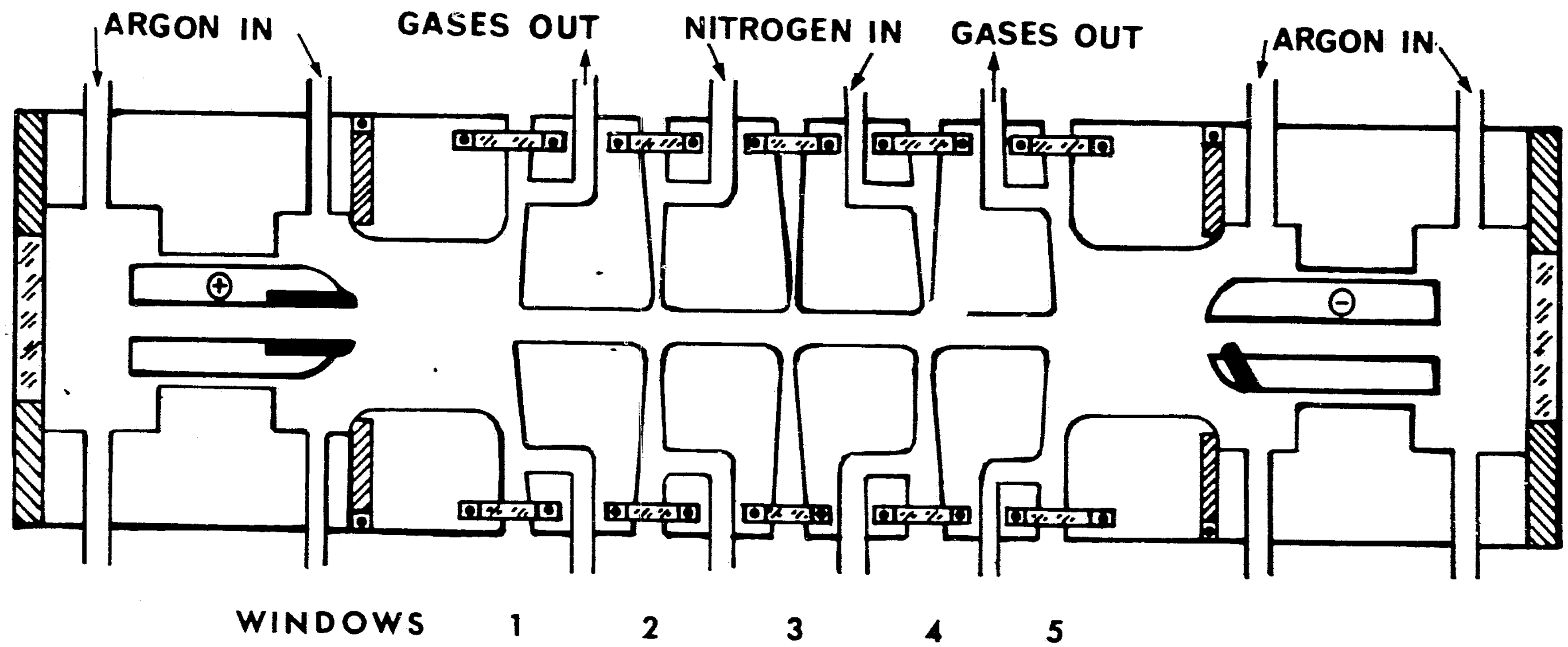

Fig. 2 Schematic of modified wall-stabilized arc.

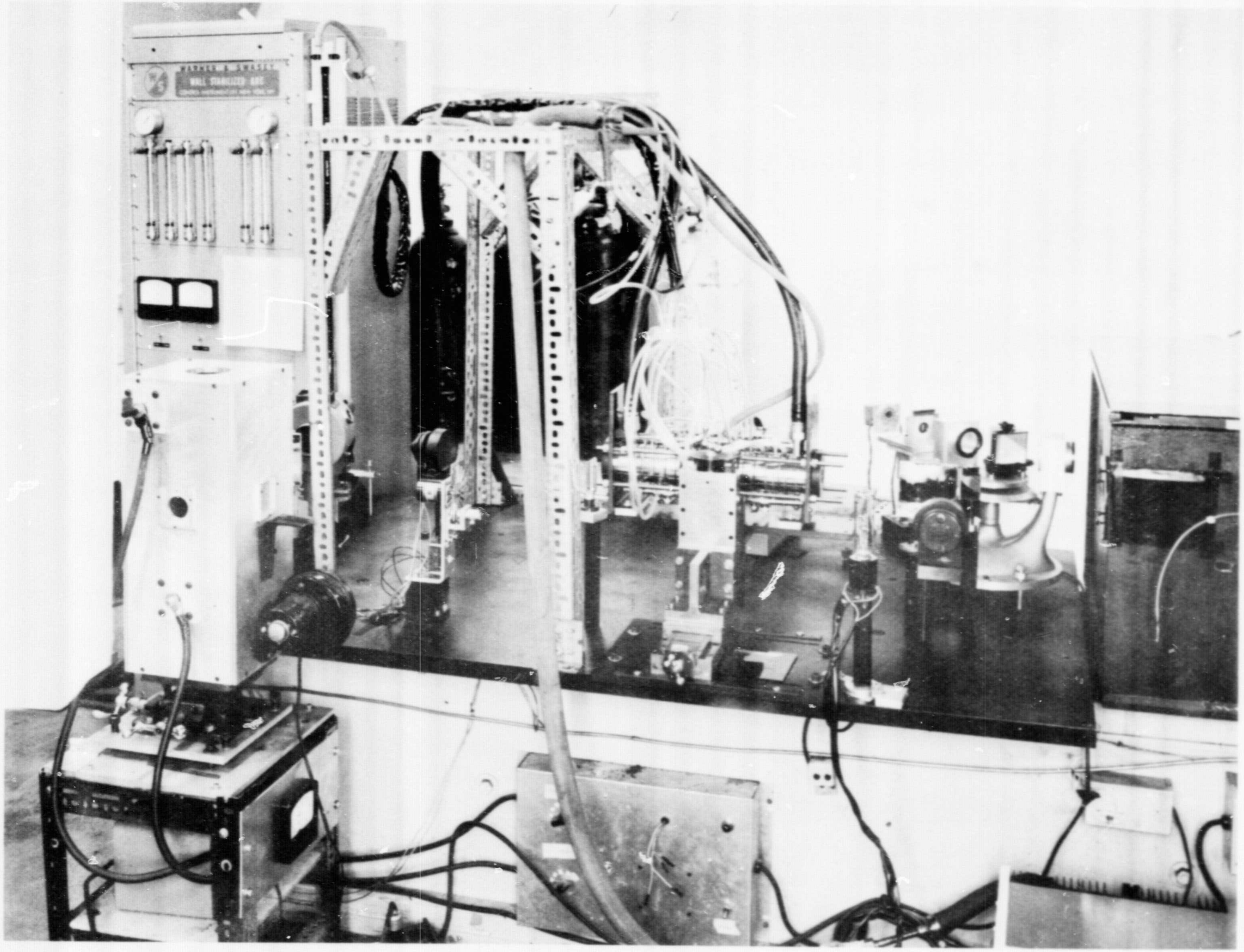

Fig. 3 Experimental set-up for emission and absorption measurements with the wall-stabilized arc.

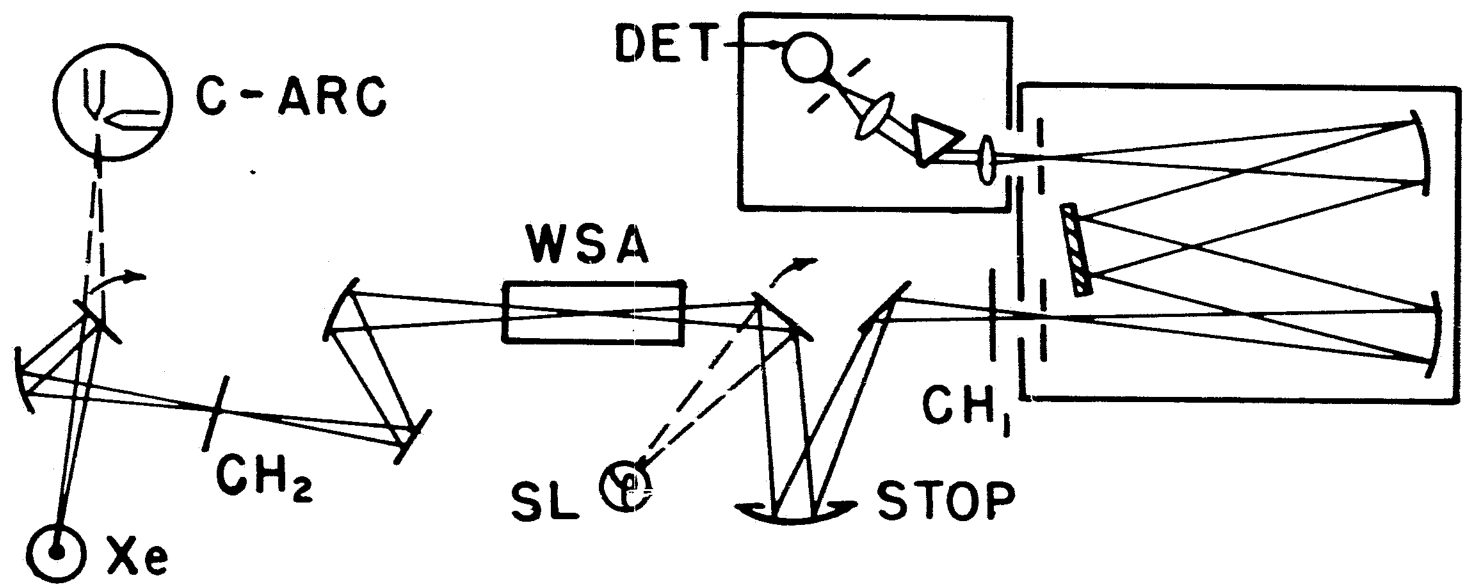

Fig. 4 Schematic of optical system used for concurrent emission-absorption measurements.

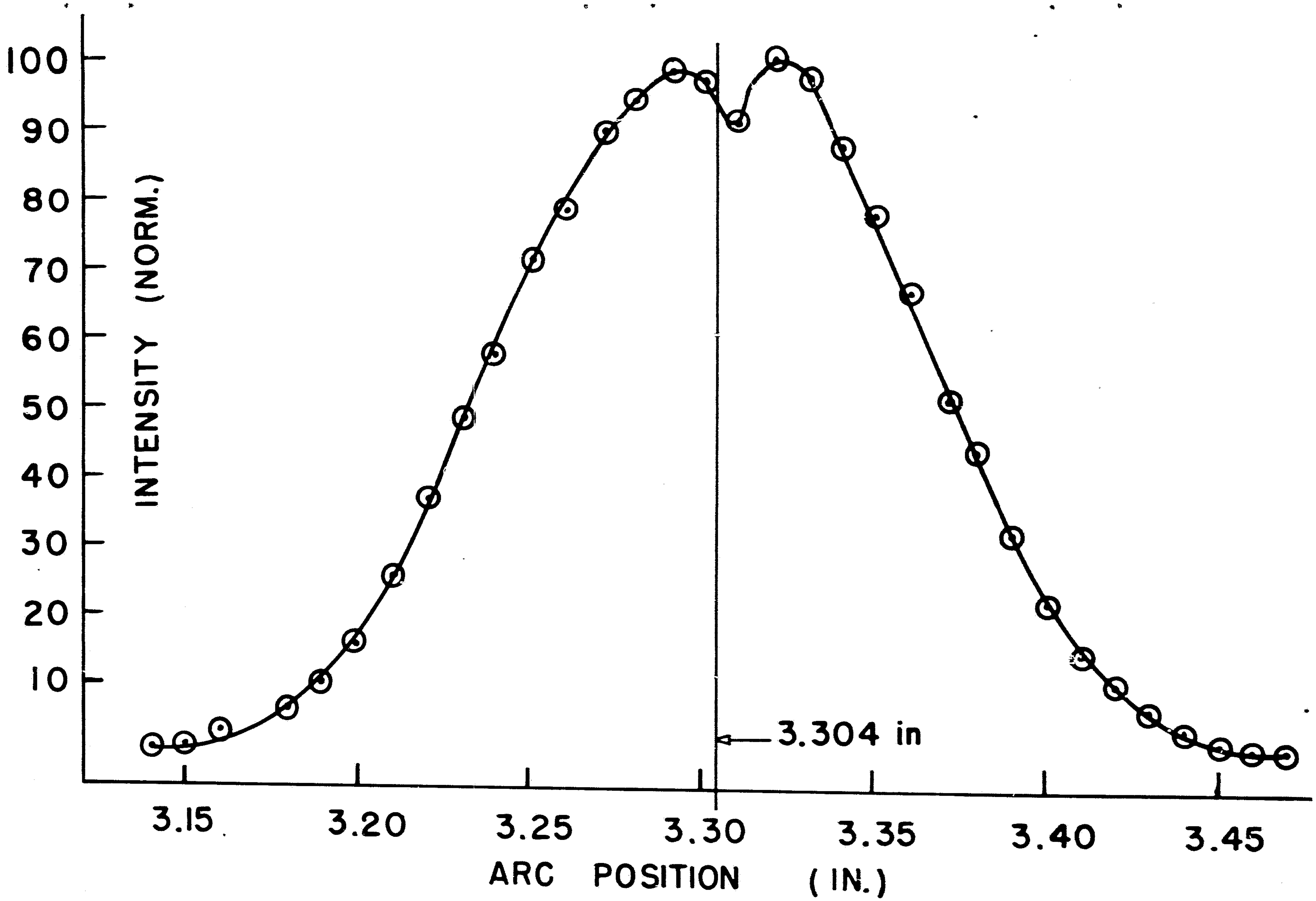

Fig. 5 Lateral intensity distribution of the continuum at 4350Å in an argon arc at 1 atm pressure and 76 ampere current.

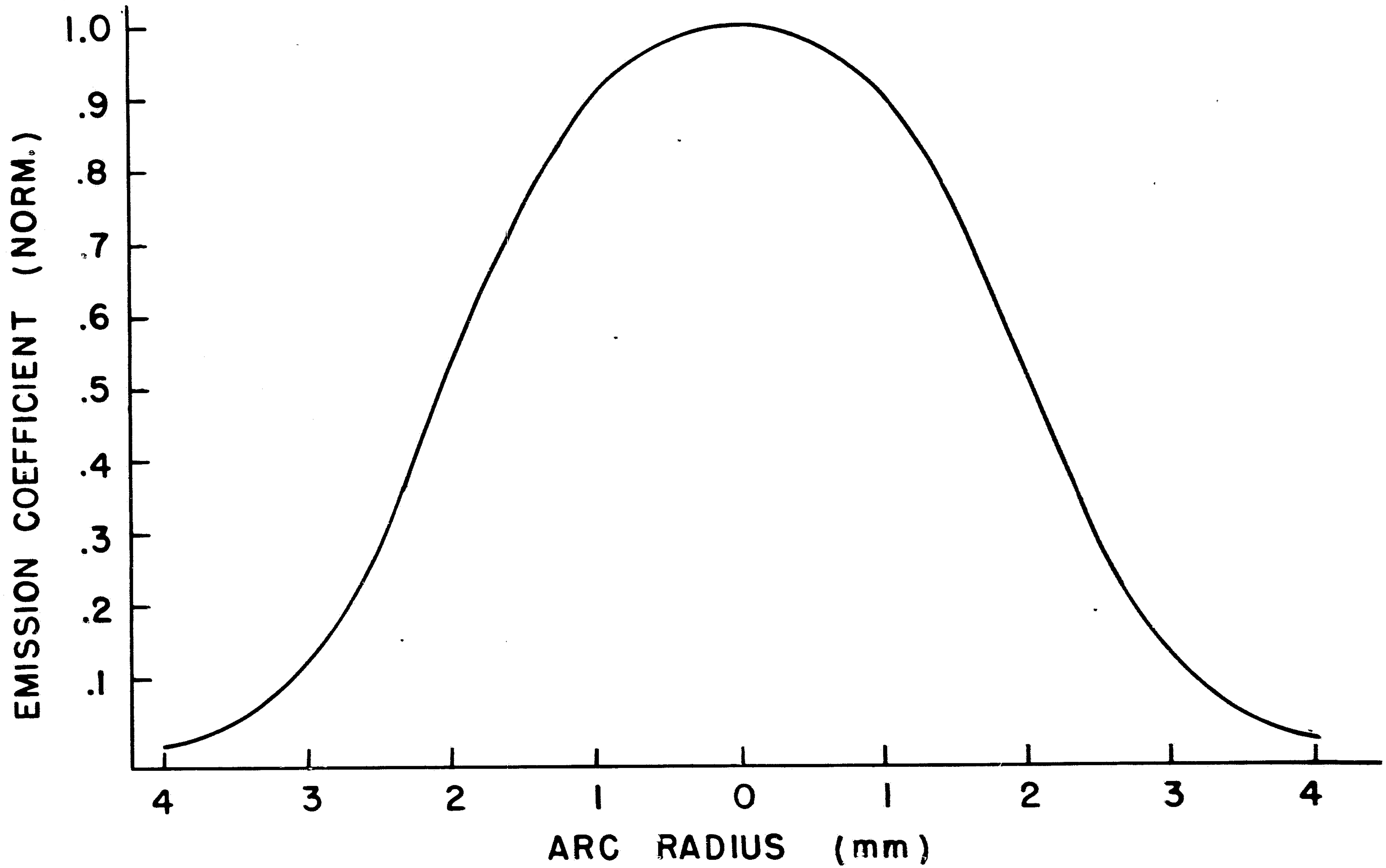

Fig. 6 Radial distribution of the emission coefficient for the continuum at 4350Å, obtained by Abel inversion of the smoothed lateral intensity distribution shown in Fig. 5.

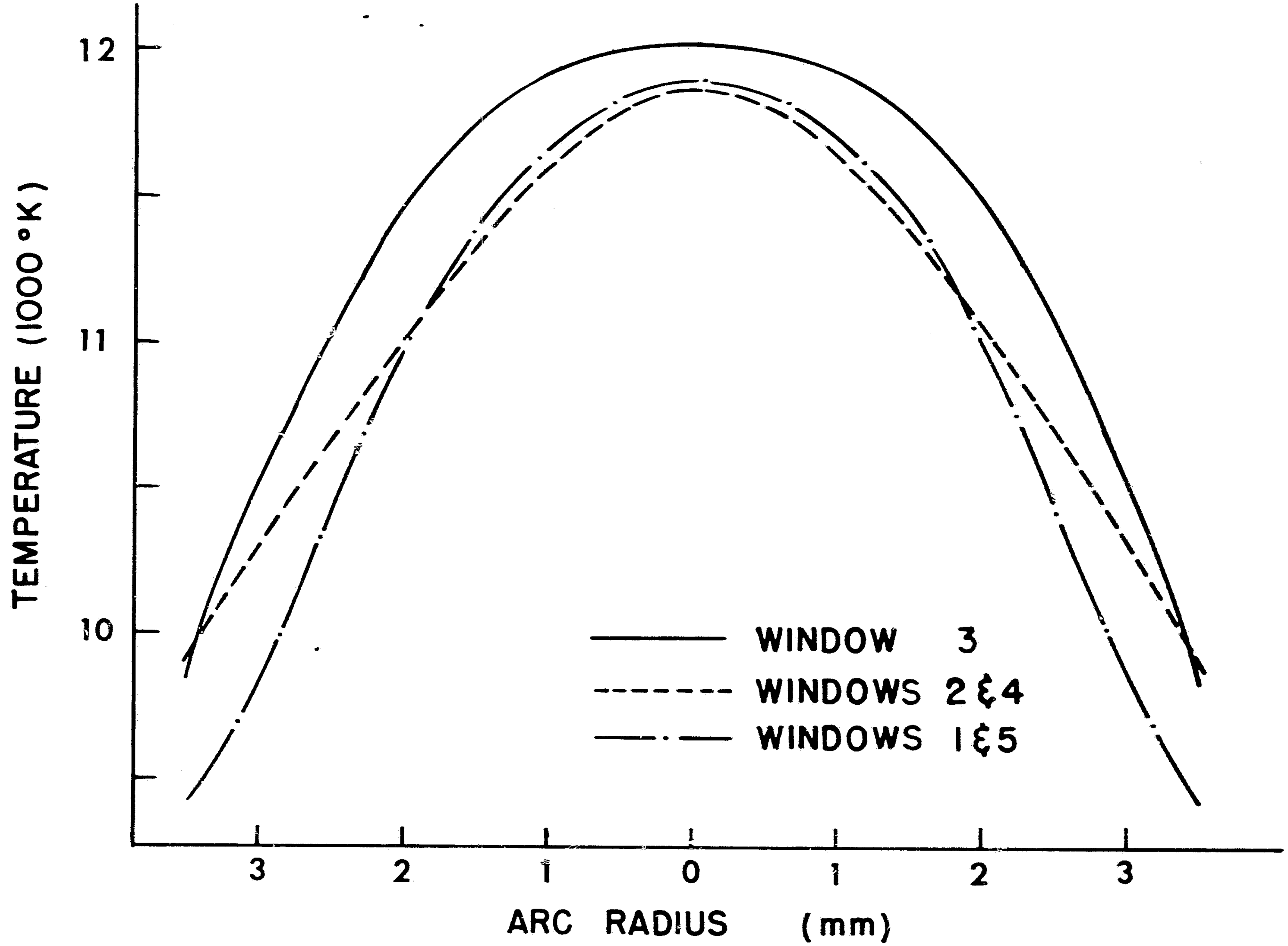

Fig. 7 Radial temperature profile at different sections of the 76 ampere atmospheric argon arc as derived from the absolute intensity of the continuum at 4350A.

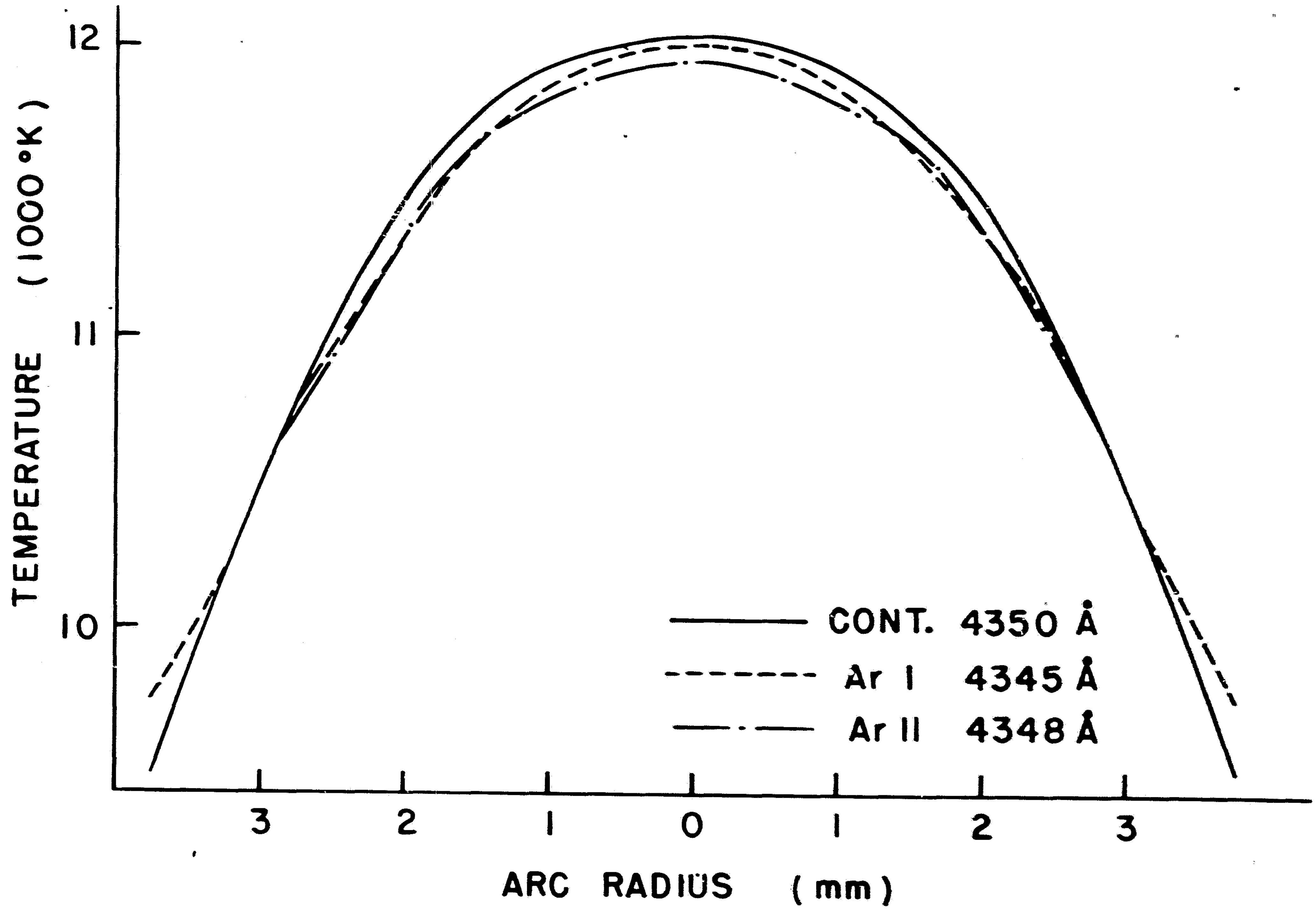

Fig. 8 Radial temperature profile of the middle section (window #3) of the 76 ampere atmospheric argon arc as determined from different spectral features.

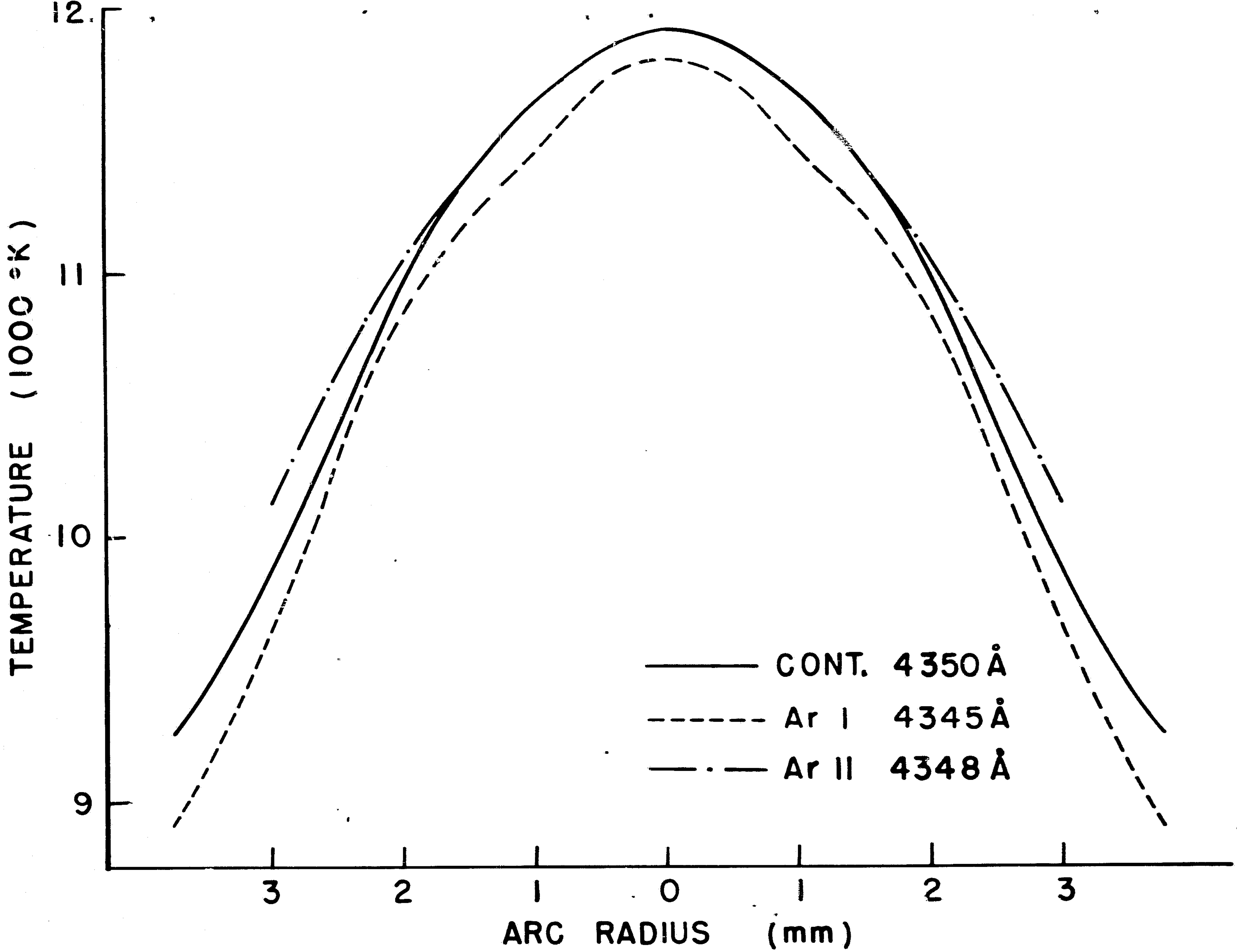

Fig. 9 Radial temperature profile at the location of window #4 of the 76 ampere atmospheric argon arc as determined from different spectral features.

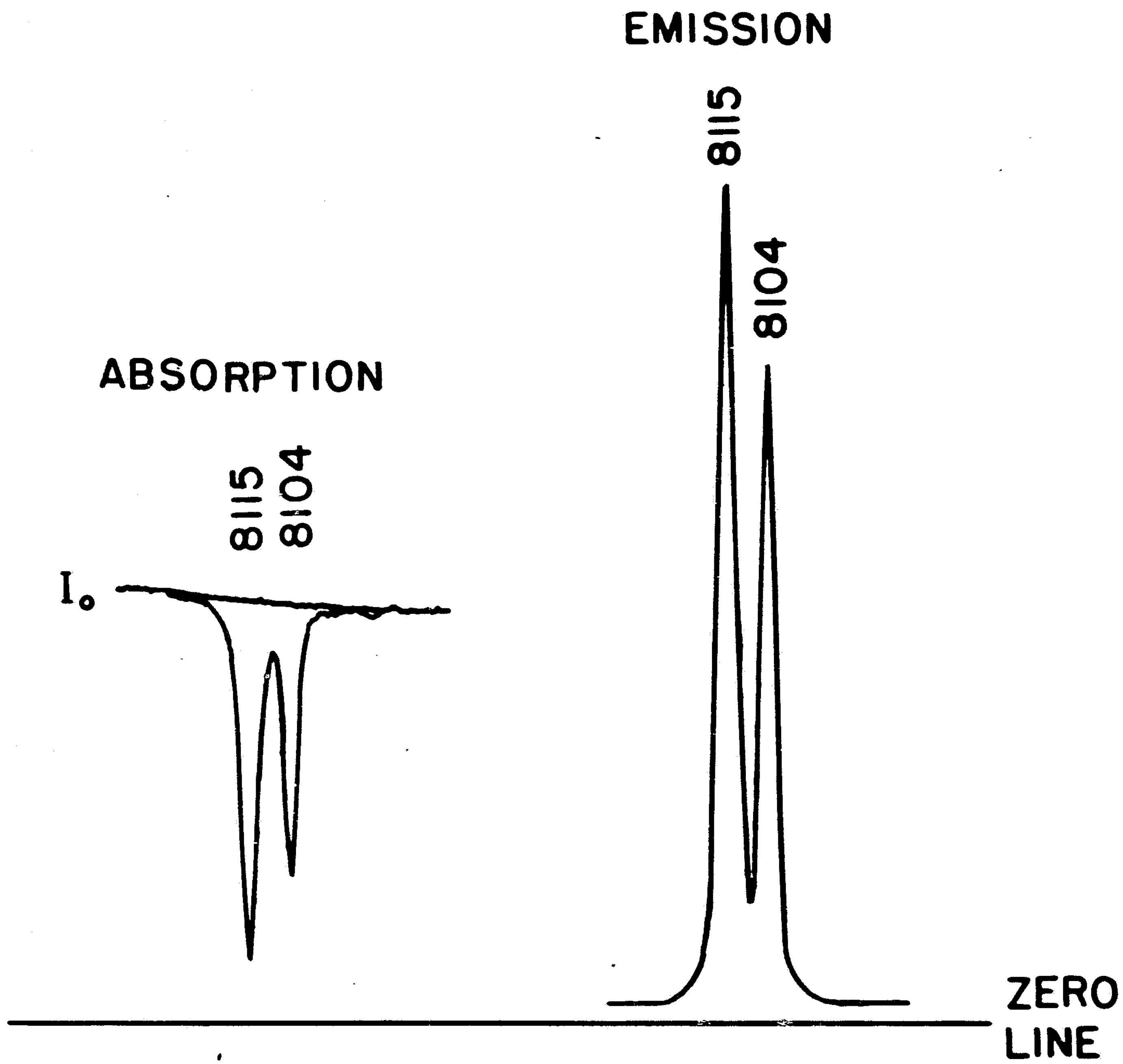

Fig. 10 Strip-chart record of an end-on measurement of the core of an atmospheric argon arc at 50 ampere.

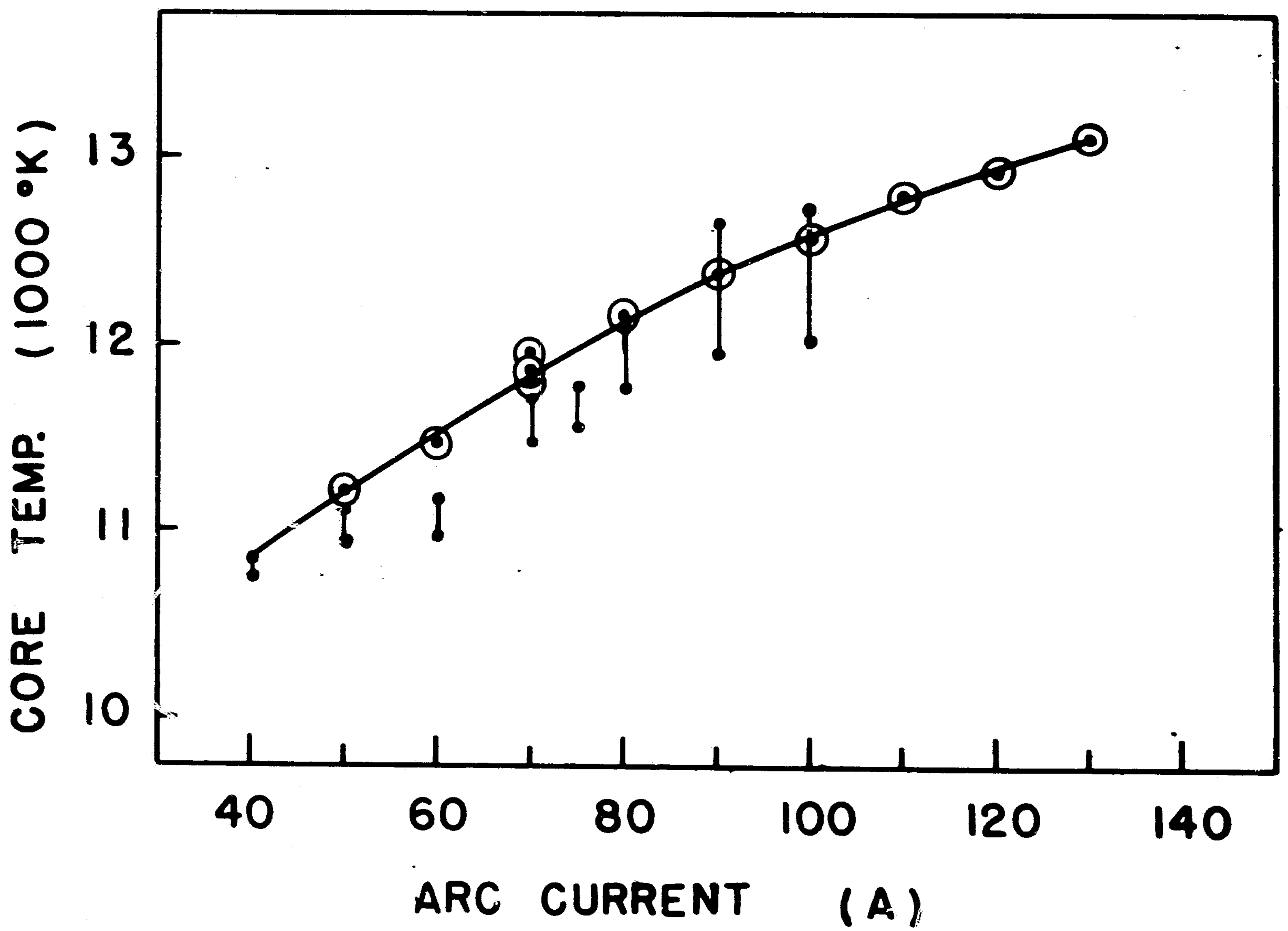

Fig. 11 Core temperature of an atmospheric argon arc at different arc currents measured in the end-on mode.

Fig. 12 Population of the upper level for the transition of Ar I 8115Å at different pressures in an argon plasma in LTE.

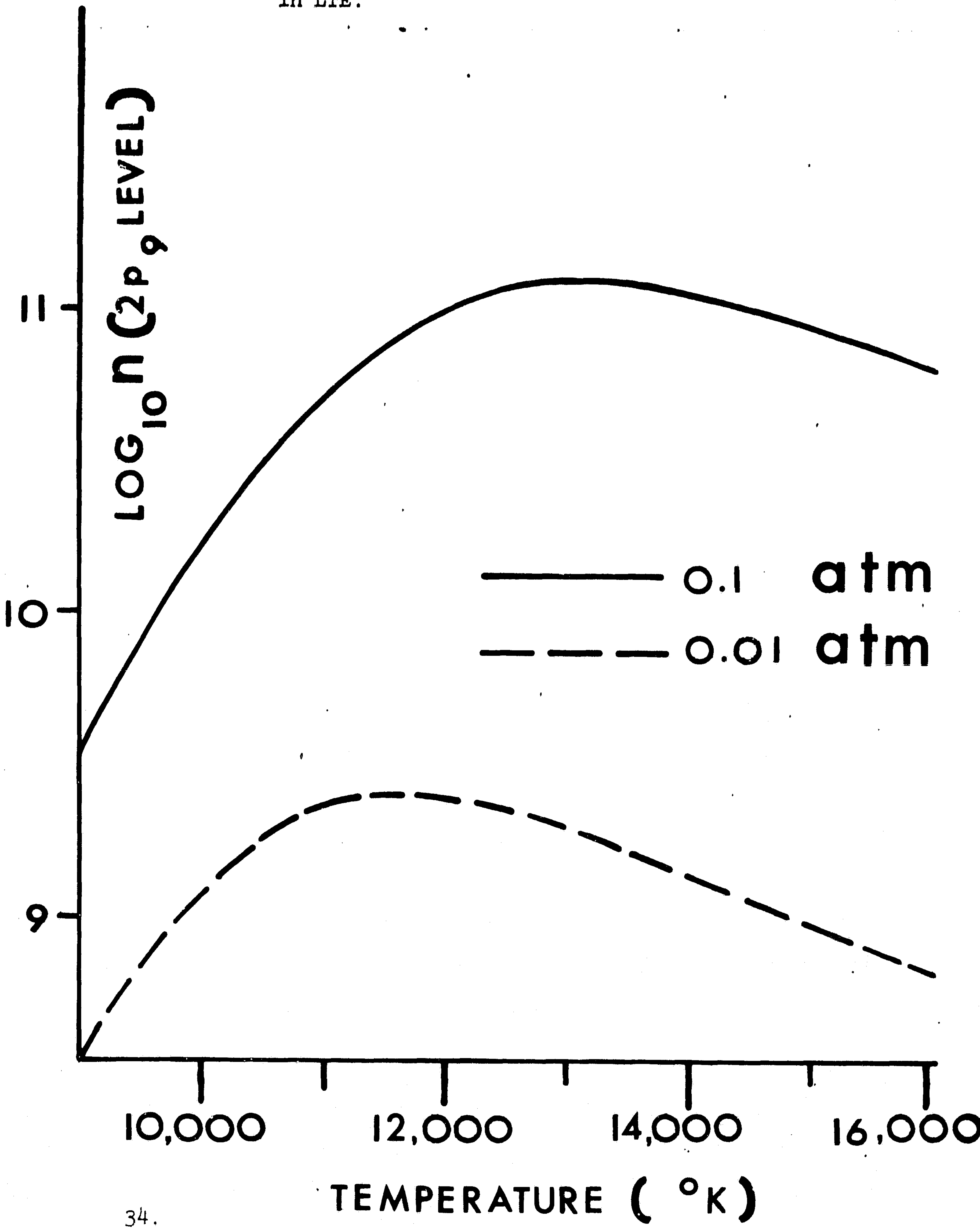

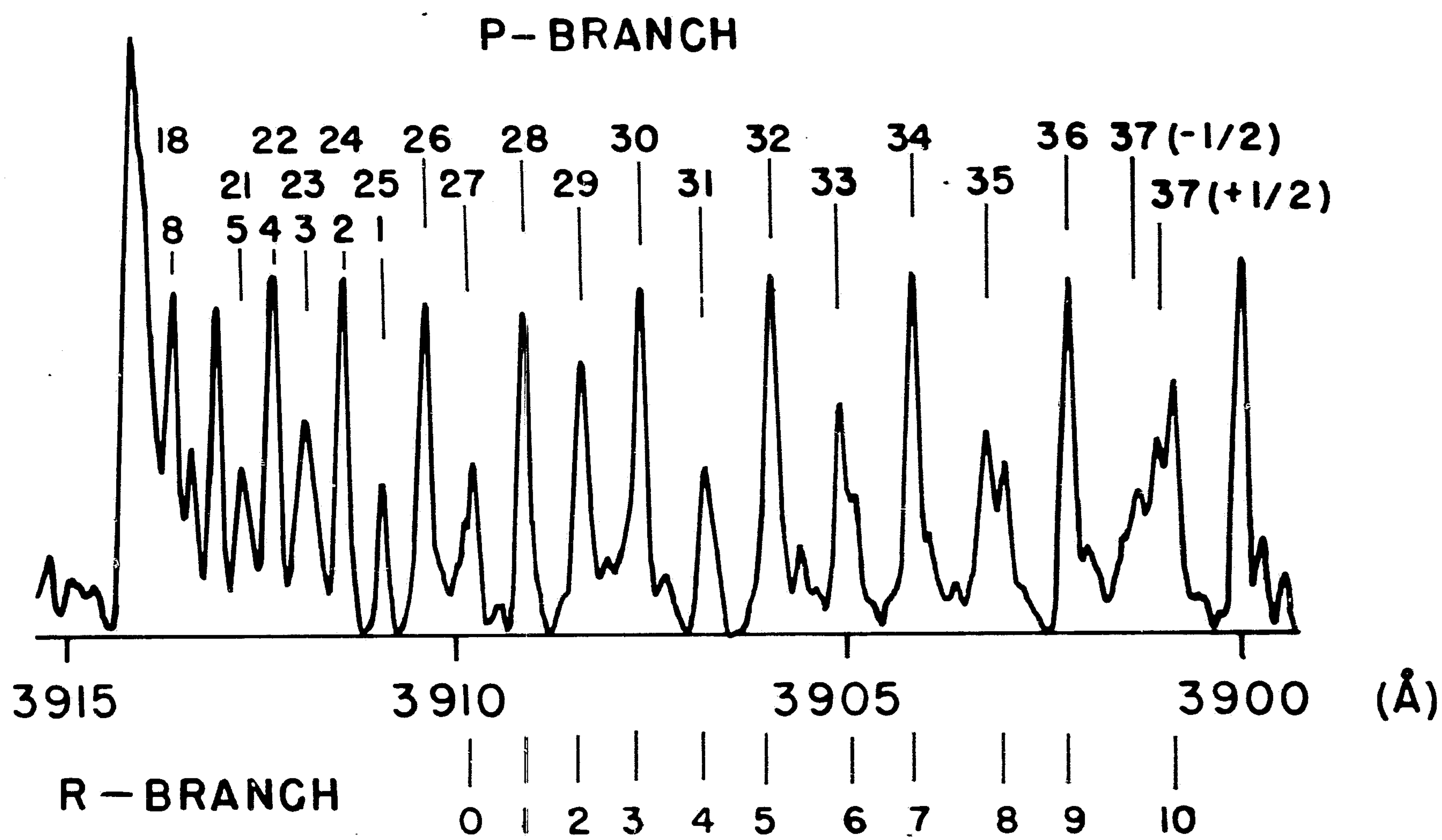

Fig. 13 Spectrum of the (0,0) N_2^+ (1st neg.) band corresponding to the core of a 40 ampere nitrogen arc at pressure of 10 torr.

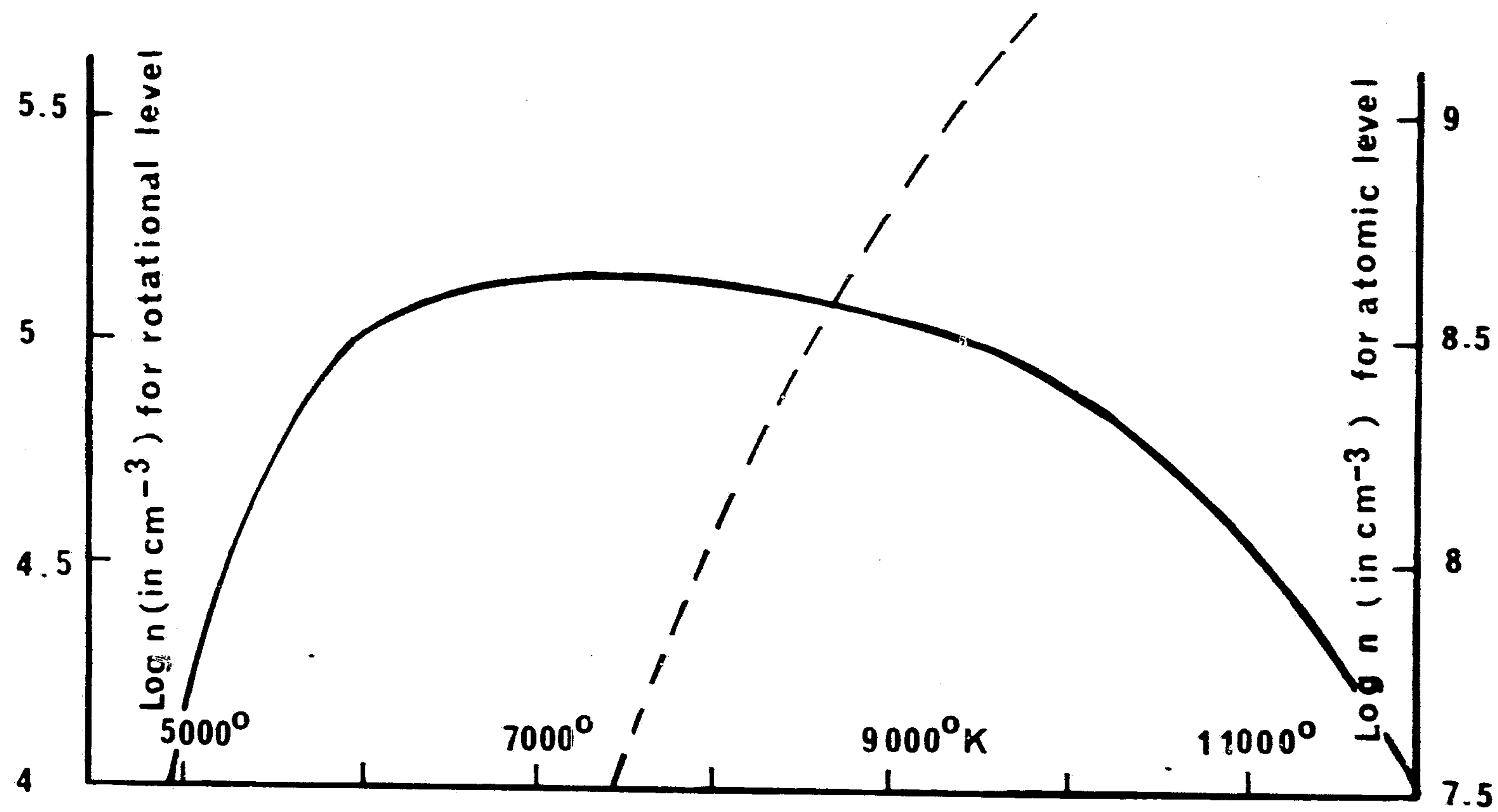

Fig. 14 Population of the upper energy level in a nitrogen plasma in LTE at a pressure of 10 torr of: a) the P-26 rotational line (solid line); and b) N I 9393Å (broken line).